DOI: 10.1002/chem.200801584

Thermal Decomposition Modes for Four-Coordinate Ruthenium Phosphonium Alkylidene Olefin Metathesis Catalysts

Erin M. Leitao,[a] Stuart R. Dubberley,[a] Warren E. Piers,*[a] Qiao Wu,[a] and Robert McDonald[b]

Abstract: The four-coordinate ruthenium phosphonium alkylidenes **1-Cy** and **1-*i*Pr**, differing in the substituent on the phosphorus center, were observed to decompose thermally in the presence of 1,1-dichloroethylene to produce $[H_3CPR_3][Cl]$. The major ruthenium-containing product was a trichloro-bridged ruthenium dimer that incorporates the elements of the 1,1-dichloroethylene as a dichlorocarbene ligand and a styrenic vinyl group on the supporting NHC ligand. Spectroscopic, kinetic, and deuterium-labeling experiments probed the mechanism of this process, which involves a rate-limiting C–H activation of an NHC mesityl *ortho* methyl group. These studies provide insight into intrinsic decomposition processes of active Grubbs type olefin metathesis catalysts, pointing the way to new catalyst design directions.

Keywords: catalysis · decomposition · kinetics · olefin metathesis · ruthenium

Introduction

Olefin metathesis is a powerful reaction mediated by homogeneous transition-metal-based catalysts.[1] The most prominent catalyst family, the Grubbs systems, are based on well-defined, five-coordinate ruthenium alkylidenes with the generalized structure shown in **I**.[2] While these are a versatile group of catalysts, challenges remain in catalyst design to produce more active, longer lived, and more selective catalysts, and work continues today in catalyst modification aimed at diversifying the Grubbs catalyst portfolio.[3]

Rational catalyst design to meet defined goals is informed by a detailed understanding of the intimate mechanism of the catalytic process and knowledge of the decomposition modes of catalyst precursors and intermediates. Generally, mechanistic information leads to ligand modification strategies to influence selectivity, while mapping decomposition pathways can suggest ways of designing more stable catalysts that exhibit improved longevity.

In the Grubbs systems **I**, much work has been done on delineating the mechanism by which they operate for olefin metathesis, including the initiation process[4] and catalyst structure–activity relationships.[5] Despite the detail available from these studies, the precise structures of many of the intermediates present in the catalytic cycle remained the domain of informed speculation based on model complexes[6] or theory.[7] The discovery of four-coordinate phosphonium alkylidene complexes[8] of general structure **II** in our laboratories has allowed a more detailed experimental examination of ruthenacyclobutane intermediates previously undetected in solution,[9,10] their dynamic behavior,[6c,11] and the mechanisms by which they interchange.[12] Thus, although work continues in this important area, excellent progress has been made in terms of our understanding of the mechanism of catalysis.

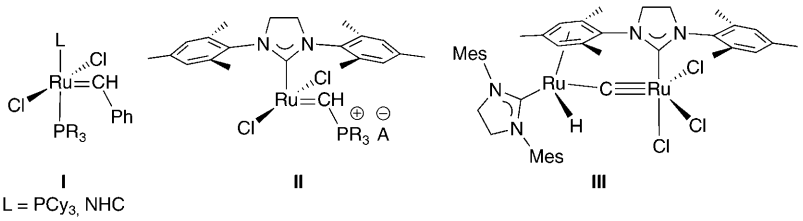

[a] E. M. Leitao, Dr. S. R. Dubberley, Prof. W. E. Piers, Dr. Q. Wu
Department of Chemistry, University of Calgary,
2500 University Dr. N.W., Calgary, AB, T2N 1N4 (Canada)
Fax: (+1) 403-289-9488
E-mail: wpiers@ucalgary.ca

[b] Dr. R. McDonald
Department of Chemistry, University of Alberta
11227 Saskatchewan Drive, Edmonton, AB, T6G 2G2 (Canada)

Supporting information for this article is available on the WWW under http://dx.doi.org/10.1002/chem.200801584.

Comparatively less detail is available regarding decomposition modes of catalyst precursors and intermediates.[13] What is known is mostly due to the isolation of ruthenium-containing decomposition products. For example, several halide-bridged dimers have been isolated and characterized,[14] suggesting the lability of the chloride ligands[15] is a potential source of catalyst death. Alternatively, ruthenium hydrido carbonyls have been isolated in reactions performed in the presence of H_2O, alcohols, or using vinyl ether substrates.[16] Other studies suggest that the aryl groups in the NHC ligands of Grubbs second-generation catalysts can undergo ring expansion in processes involving the ruthenium alkylidene.[17] In a comprehensive study, Grubbs and co-workers have determined that a major decomposition pathway for generation 1 and 2 catalysts involves the attack of free phosphine (formed in the initiation step) on a $Ru{=}CH_2$ group, leading to loss of $[H_3CPR_3][Cl]$ and formation of the carbide-bridged dimer **III**.[18] This study clearly shows that the presence of free phosphine not only stunts activity, it can affect overall catalyst turnovers due to its role in the catalyst decomposition process.

While the phosphonium alkylidenes **II** are quite thermally robust in the solid state and in solution under ambient conditions, they do decompose in solution at elevated temperatures. As such, they present an opportunity to study the decomposition modes of four-coordinate ruthenium alkylidenes in the absence of free phosphine. The compounds **1-Cy** and **1-*i*Pr** are exceptionally active olefin metathesis catalysts by virtue of their rapid initiation kinetics, but they do suffer from low turnovers due to their moderate thermal instability at low olefin concentrations. Although this likely reflects the intrinsic instability of the 14-electron methylidene species or ruthenacyclobutane resting states present during catalysis,[9,11,12] an analysis of the decomposition modes of the catalyst precursors **1-Cy** and **1-*i*Pr** may provide some insight into the low-energy decomposition pathways available to catalytic intermediates. Here we describe the pathways by which these compounds decompose.

Results and Discussion

The phosphonium alkylidene complexes **1-Cy** and **1-*i*Pr**, differing only in the steric bulk associated with the phosphonium moiety, were prepared as previously described.[8a,11] The less bulky isopropyl-substituted derivative is best prepared and stored as its zwitterionic chloride salt **1-*i*Pr-Cl**;[19] the chloride ligand *trans* to the NHC ligand is readily abstracted by $B(C_6F_5)_3$[20] to form **1-*i*Pr** partnered with the $[ClB(C_6F_5)_3]$ ion. For consistency in the mechanistic studies described here, both **1-Cy** and **1-*i*Pr** were generated by this method (Scheme 1) from the zwitterionic trichlorides.

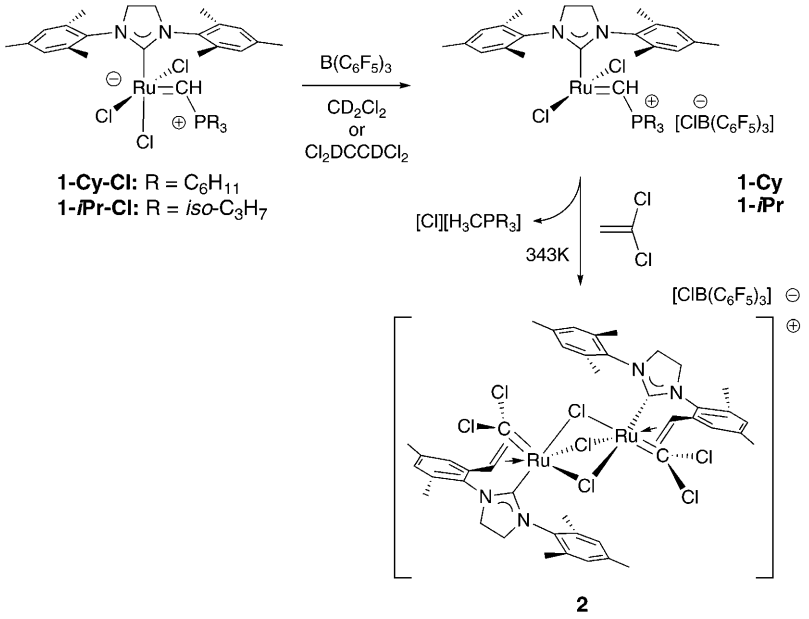

Scheme 1. Thermal decomposition of ruthenium phosphonium alkylidene olefin metathesis catalysts.

Qualitatively, compounds **1-R** are reasonably thermally stable in solution at room temperature, with half-lives on the order of hours. However, heating to 70°C leads to more rapid decomposition. Monitoring such processes by ^1H and ^{31}P NMR spectroscopy indicates that there are several ruthenium-containing products, but that there is one phosphorus-containing product formed cleanly, namely the methyl phosphonium salts $[MePR_3]^+[Cl]^-$. These products were easily identified by their characteristic ^{31}P NMR chemical shifts ($\delta = 34.6$ and 45.6 ppm in CD_2Cl_2 for R = Cy and *i*Pr, respectively), ESI mass spectrometric data (*m*/*z* 295 and 175), and separate syntheses.

In an attempt to identify the ruthenium-containing product(s), the compounds were allowed to decompose in the presence of various trapping agents. The most successful was 1,1-dichloroethylene, an olefin well known to be a poor substrate for metathesis.[21] Indeed, this substrate is unreactive towards both **1-Cy** and **1-*i*Pr** in dichloromethane,[22] but when allowed to decompose in its presence, compounds **1-R** again produce $[MePR_3]^+[Cl]^-$ cleanly along with a predominant ruthenium-containing product, in approximately 40–45% yield based on NMR spectroscopy. X-ray quality crystals of this material were obtained from the crude reaction mixture and its structure was determined.

This analysis revealed its structure to be the cationic trichloride bridged dimer shown in Scheme 1, which includes a dichlorocarbene ligand at each Ru center and a modified NHC ligand wherein one of the *ortho* mesityl methyl groups has been homologated into a vinyl group that coordinates the Ru center. A thermal ellipsoid diagram of the cationic portion of the ion pair is shown in Figure 1; here, the crystals were obtained from the experiment utilizing **1-Cy** partnered with the $[B(C_6F_5)_4]^-$ ion, but **2** is produced in similar amounts regardless of the anion. Notable features of the structure are as follows. The two halves of the dimer are related by a C_2 axis that bisects the Ru-Cl1-Ru' angle and runs through the centroid of the Ru-Cl2-Ru′-Cl2′ ring. The Ru centers are distorted octahedral in geometry, joined through the face formed by the three bridging chlorides. The three Ru–Cl distances are slightly different due to the three different *trans* ligands. The trapping 1,1-dichloroethylene reagent has been split into a dichlorocarbene ligand, with a short Ru–C1 distance of 1.844(3) Å, whereas the $=CH_2$ group has been added to an *ortho* methyl group of an NHC mesityl substituent, forming a styrenic group that now coordinates the ruthenium center in an unsymmetrical fashion, the terminal carbon C20 being more closely associated with the ruthenium (2.209(3 Å) than C19 (2.255(3 Å).

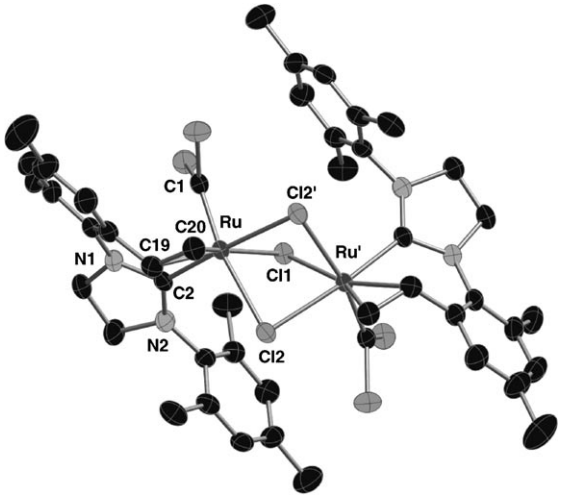

Figure 1. Thermal ellipsoid diagram (50%) of the cationic portion of **2**; the counteranion is $[B(C_6F_5)_4]^-$. Selected bond lengths [Å]: Ru–Cl1 2.4201(7), Ru–Cl2 2.4982(8), Ru–Cl2′ 2.4951(7), Ru–C1 1.844(3), Ru–C2 2.065(2), Ru–C19 2.255(3), Ru–C20 2.209(3), C19–C20 1.388(5). Selected non-bonding distance [Å]: Ru–Ru′ 3.29. Selected bond angles [°]: C1-Ru-Cl2 169.35(9), C1-Ru-Cl1 93.40(9), C1-Ru-Cl2′ 90.01(9), C1-Ru-C2 90.63(12), C2-Ru-Cl1 91.87(8), C2-Ru-Cl2′172.39(8), C2-Ru-Cl2 98.23(9), Cl1-Ru-Cl2 80.47(2), Cl1-Ru-Cl2′ 80.44(3), Cl1-Ru-C19 163.51(8), Cl1-Ru-C20 155.93(9), Ru-Cl1-Ru′ 85.66(3), Ru-Cl2-Ru′ 82.45(2).

The Ru centers are distorted octahedral in geometry, joined through the face formed by the three bridging chlorides. The three Ru–Cl distances are slightly different due to the three different *trans* ligands. The trapping 1,1-dichloroethylene reagent has been split into a dichlorocarbene ligand, with a short Ru–C1 distance of 1.844(3) Å, whereas the $=CH_2$ group has been added to an *ortho* methyl group of an NHC mesityl substituent, forming a styrenic group that now coordinates the ruthenium center in an unsymmetrical fashion, the terminal carbon C20 being more closely associated with the ruthenium (2.209(3 Å) than C19 (2.255(3 Å).

Spectroscopic data for **2** is completely consistent with the structure as determined by X-ray crystallography. Proton and ^{13}C NMR analysis of isolated crystals indicates the desymmetrization of the NHC ligand as exemplified by the five separate resonances for mesityl methyl groups observed in both spectra. Characteristic resonances for a coordinated vinyl group are also present, with typical coupling patterns observed in the ^1H NMR spectra. In the ^{13}C NMR spectrum, a weak resonance at $\delta = 265.02$ ppm is assignable to the dichlorocarbene carbon atom.[23] Finally, ESI mass spectrometric analysis of **2** gave a parent ion for $C_{46}H_{52}Cl_7N_4Ru_2^+$ (m/z 1111) with an isotope peak pattern that matched the calculated distribution for this empirical formula.

Since the primary ruthenium-containing product in this decomposition is dimeric, the reaction order in [Ru] was examined by following the loss of compounds **1-R** using ^1H and/or $^{31}P\{^1H\}$ NMR spectroscopy. The plots in Figure 2a give excellent first-order fits, and show that the phosphonium alkylidene with the less bulky $P(iPr)_3$ group decomposes with a rate constant about an order of magnitude faster than **1-Cy** (all rate constants determined are tabulated in Table 1). Furthermore, the decomposition of **1-*i*Pr** at various $[Ru]_0$ at 330 K (Figure 2b) also show that the process is first-order in [Ru]. As shown in Figure 3, Eyring analysis of the rate constants for the disappearance of **1-*i*Pr** at various temperatures surrenders activation parameters of $\Delta H^{\ddagger} = 64(2)$ kJ mol^{-1} and $\Delta S^{\ddagger} = -129(5)$ J K^{-1} mol^{-1}.

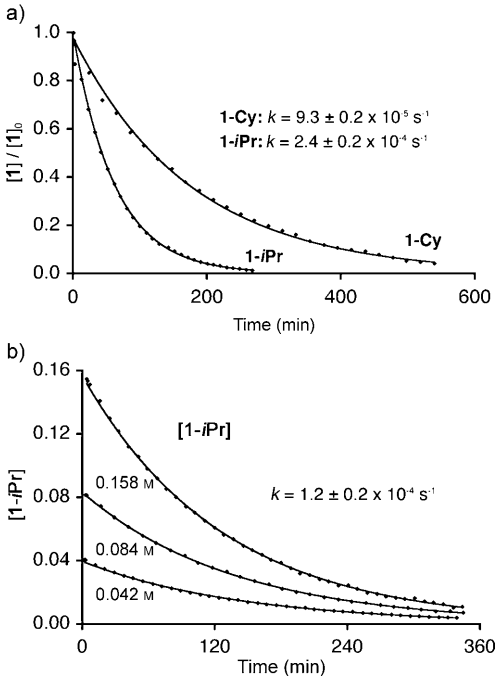

Figure 2. a) Exponentially fitted first-order plots for disappearance of **1-Cy** and **1-*i*Pr** at 343 K. b) Exponentially fitted first-order plots for disappearance of **1-*i*Pr** at 330 K using various initial concentrations of **1-*i*Pr**.

A plausible mechanism that accounts for these observations is given in Scheme 2. Since the reaction is first-order in [Ru], and compounds **1-R** do not react with 1,1-dichloroethylene under the conditions of decomposition, the rate-limiting step is likely an intramolecular process, which produces a reactive intermediate that is trapped by the olefin to eventually give **2**. We propose that this step involves activation of a C–H bond of an *ortho* methyl group of one of the

Table 1. Rate constants for the decomposition of **1-Cy** and **1-*i*Pr** at different concentrations and temperatures.

Entry	Compound	[Ru] [M]	Temp [K]	Rate constant[c] [s^{-1}]
1	**1-Cy**	0.069	324	1.5×10^{-5}
2	**1-Cy**	0.069	334	3.6×10^{-5}
3	**1-Cy**	0.069	345	8.6×10^{-5}
4	**1-Cy**	0.069	354	2.0×10^{-4}
5	**1-Cy**	0.069	365[a]	3.9×10^{-4}
6	**1-Cy**	0.069	343	9.3×10^{-5}
7	[D_{22}]-**1-Cy**	0.069	343	2.1×10^{-5}
8	[D_{11}]-**1-Cy**	0.069	343	4.8×10^{-5}
9	[D_6]-**1-Cy**	0.069	343	4.9×10^{-5}
10	**1-*i*Pr**	0.042	330	1.1×10^{-4}
11	**1-*i*Pr**	0.084	330	1.2×10^{-4}
12	**1-*i*Pr**	0.158	330	1.3×10^{-4}
13	**1-*i*Pr**	0.084	313	2.6×10^{-5}
14	**1-*i*Pr**	0.084	320	5.8×10^{-5}
15	**1-*i*Pr**	0.084	344	2.8×10^{-4}
16	**1-*i*Pr**	0.084	355[b]	5.9×10^{-4}
17	**1-*i*Pr**	0.080	343	2.4×10^{-4}
18	[D_{22}]-**1-*i*Pr**	0.080	343	5.1×10^{-5}
19	[D_{11}]-**1-*i*Pr**	0.080	343	1.4×10^{-4}
20	[D_6]-**1-*i*Pr**	0.080	343	1.6×10^{-4}

[a] Entries 1–5 used in a Eyring plot to give $\Delta H^{\ddagger}=76(2)$ kJ mol^{-1}; $\Delta S^{\ddagger}=-104(5)$ J K^{-1} mol^{-1}. [b] Entries 11, 13–16 used in a Eyring plot to give $\Delta H^{\ddagger}=64(2)$ kJ mol^{-1}; $\Delta S^{\ddagger}=-129(5)$ J K^{-1} mol^{-1}. [c] Error in rate constant measurements is $\pm0.2\times10^{-4}$ or $\pm0.2\times10^{-5}$ depending on the value.

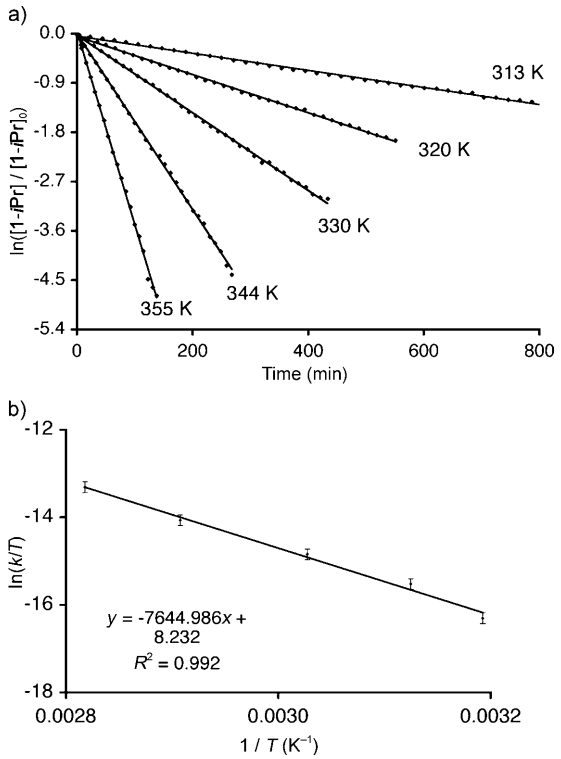

Figure 3. a) Logarithmic first-order plots for the disappearance of **1-*i*Pr** (0.084 M) at various temperatures. See Table 1 for first-order rate constants. b) Eyring plot for the decomposition of **1-*i*Pr**. See text and Table 1 for activation parameters.

mesityl substituents, possibly via addition across the Ru=C phosphonium alkylidene bond.[24] The resulting (formally) Ru^{IV} intermediate **IV** rapidly eliminates the observed

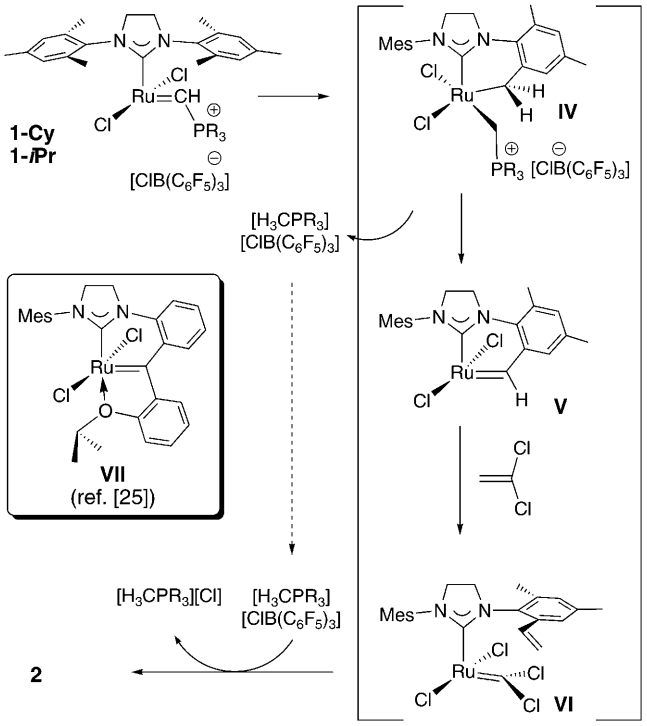

Scheme 2. Proposed mechanism of decomposition for phosphonium alkylidene complexes **1-R**.

methyl phosphonium product via what is essentially the reverse of the initial step, that is, C–H bond formation via α elimination, to give the chelated alkylidene complex **V**. This highly reactive species undergoes cross metathesis with the trapping olefin in a step that institutes both the dichlorocarbene unit and the styrenic vinyl group observed in the final product **2**. Intermediate **VI** thus formed undergoes dimerization after loss of chloride; ion exchange yields the observed products **2** and $[H_3CPR_3][Cl]$.

None of the proposed intermediates **IV**–**VI** are observed directly, but some precedent and evidence for **V** is available. Blechert and co-workers have reported a chelated alkylidene complex (**VII**, Scheme 2) derived from air oxidation of NHC-supported Grubbs–Hoveyda type catalysts with *N*-phenyl substitution on the NHC donor.[25] While the proposed mechanism of formation of the Blechert compound is quite different, and it is "completely inactive" as an olefin metathesis initiator, it serves as an excellent structural model for the proposed intermediate **V**.

Evidence for the viability of **V** is provided by monitoring the decomposition of **1-*i*Pr** as its triflate salt[26] (or **1-*i*Pr** itself) in the *absence* of any trapping agent at room temperature. Over 1–2 days at room temperature, a species assigned as the mixed dimer **3** grows in until it comprises about 20% of the ruthenium speciation, the remainder being unreacted **1-*i*Pr-X** and a small amount (<5%) of other, unidentified alkylidene-containing species. Compound **3** is formed by the "self trapping" of **V** by **1-*i*Pr-X**; under the conditions of its generation, it decomposes further, but cooling enriched sam-

ples to −53°C allows partial analysis of its ^{1}H and ^{13}C NMR spectra.

In the alkylidene region of the ^{1}H NMR spectrum (using **1-*i*Pr-OTf**), two new signals in a 1:1 ratio at $\delta = 20.23$ ppm ($^{2}J_{H,P} = 46$ Hz) and $\delta = 18.57$ ppm (singlet) are assignable to the phosphonium alkylidene and the chelated alkylidene groups of **3**, respectively (see inset, Scheme 3). The magnitude of $^{2}J_{H,P}$ in the former resonance is indicative of a five-coordinate ruthenium center; these couplings are about 37 Hz in the four-coordinate phosphonium alkylidenes. These resonances correlate with ^{13}C signals at $\delta = 292.3$ ppm ($^{1}J_{C,H} = 166 \pm 4$ Hz, c.f. 168 Hz for the starting material phosphonium alkylidene) and $\delta = 303.3$ ppm ($^{1}J_{C,H} = 156 \pm 4$ Hz), characteristic of alkylidene carbon atoms.[27] Unfortunately, all attempts to isolate **3** failed due to its propensity to undergo further decomposition. Furthermore, attempts to functionalize **3** via reaction with external bases such as PCy_3 or pyridine, so as to isolate a derivative, result in the trapping of the starting complexes **1**. It should be noted, however, that precedent exists for the trapping of Grubbs framework 14-electron alkylidene complexes by $LMCl_2$ compounds (M = Ru, Os) to give dichloro-bridged dimers similar in character to **3**.[28]

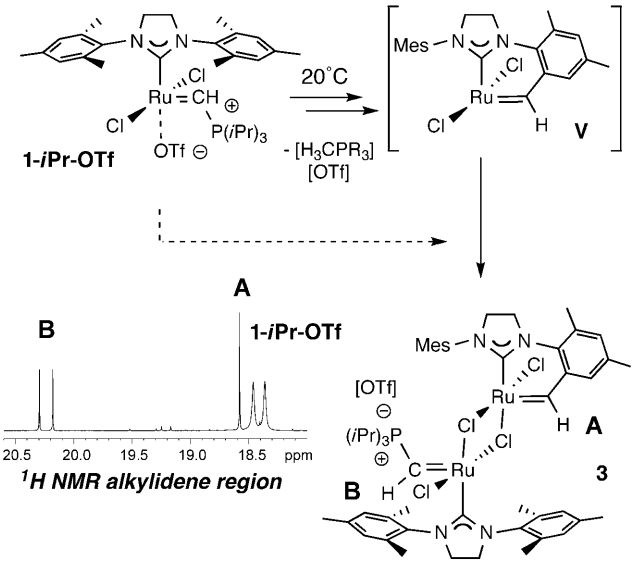

Scheme 3. Self-trapping of the proposed intermediate **V**.

Further support for the mechanistic proposals was garnered by selective deuterium-labeling and the determination of inter- and intramolecular kinetic isotope effects (Figure 4 and Table 2). Since activation of a benzylic C–H bond of an *ortho* methyl group of an NHC mesityl moiety appears to be rate-limiting, three deuterated isotopomers of each phosphonium alkylidene were prepared in which these methyl groups were either fully ([D_{22}]-**1-R**) or partially deuterated. The partially deuterated were subdivided into [D_{11}]-**1-R** or [D_6]-**1-R** isotopomers with label incorporation as shown. The fully deuterated isotopomers were used to determine

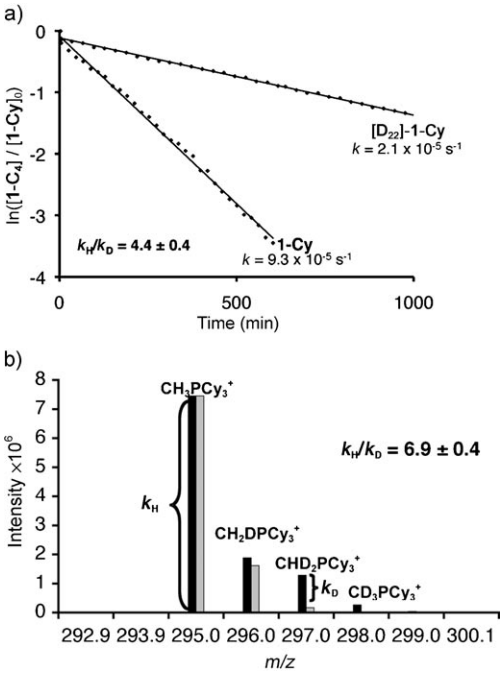

Figure 4. a) Representative intermolecular kinetic isotope effect based on logarithmic first-order plots for the decomposition of **1-Cy** and [D_{22}]-**1-Cy** at 343 K (determined by NMR). The ratio of k(**1-Cy**) to k([D_{22}]-**1-Cy**) gives the intermolecular KIE of 4.4(4). b) Representative intramolecular kinetic isotope effect based on the final decomposition mixture of [D_{11}]-**1-Cy** at 343 K (determined by ESI MS). The ratio of m/z 295 ($CH_3PCy_3^+$) over corrected m/z 297 ($CHD_2PCy_3^+$); gives an intramolecular KIE of 6.9(4), where the correction is the natural isotopic distribution (gray bars) of the parent ion (m/z 295) against the experimental spectrum (black bars).

Table 2. Inter- and intramolecular kinetic isotope effects for the decomposition of isotopomers of **1-Cy** and **1-*i*Pr**.

Type of competition	Compounds	k_H/k_D[c] (±0.4)
intermolecular[a]	**1-Cy**/[D_{22}]-**1-Cy**	4.4
intramolecular[b]	[D_{11}]-**1-Cy**	6.9
intramolecular[b]	[D_6]-**1-Cy**	6.8
intermolecular[a]	**1-*i*Pr**/[D_{22}]-**1- *i*Pr**	4.7
intramolecular[b]	[D_{11}]-**1- *i*Pr**	6.2
intramolecular[b]	[D_6]-**1-*i*Pr**	5.9

[a] Measured by comparing the rate constants obtained by NMR (entries 6/7 and 17/18 of Table 1). [b] Measured by comparing the intensities of isotopomers by ESI MS. [c] All decompositions were performed at 343 K; **1-*i*Pr** complexes were 0.080 M in Ru and **1-Cy** complexes were 0.069 M in Ru.

the intermolecular isotope effects using NMR spectroscopy; Figure 4a shows a representative kinetic plot. The partially deuterated compounds were used to determine intramolecular k_H/k_D values by quantitatively assessing the ratio of $[H_3CPR_3]^+$ and $[HD_2CPR_3]^+$ isotopomers in the methylphosphonium salt product by using ESI mass spectrometry. Figure 4b shows a representative mass spectrum; full details of how these spectra were calibrated and corrected for natural abundance isotopomers is given in the Supporting Information. Consistent with our mechanistic proposal, these are the two predominant isotopomers observed; less than 2%

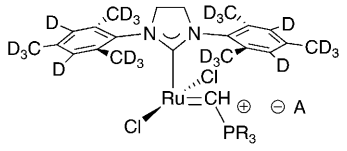

[D_{22}]-**1-R**

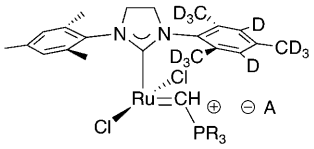

[D_{11}]-**1-R**

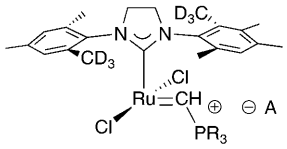

[D_6]-**1-R**

of the $[H_2DCPR_3]^+$ isotopomer was present and likely due to the less than complete labeling of the starting material, which was available 98% deuterated. Furthermore, no deuterium incorporation into the phosphonium alkylidene position was observed during any of these reactions, suggesting that the C–H activation and $[H_3CPR_3]^+$ elimination steps are indeed irreversible as suggested in Scheme 2.

As Figure 4 and Table 2 indicate, there is a substantial intermolecular isotope effect of $k_H/k_D = 4.4(4)$ for **1-Cy**/[D_{22}]-**1-Cy** and 4.7(4) for **1-*i*Pr**/[D_{22}]-**1-*i*Pr**. These are large effects considering that the kinetic measurements are made at 343 K. The intramolecular isotope effects are also large and, surprisingly, larger than the intermolecular k_H/k_D values by about 1–3. These differences are reproducible and not due to the different techniques used to evaluate them; the measured intramolecular k_H/k_D for [D_{11}]-**1-Cy** using ESI MS methodology (6.9) is in agreement with the value of 6.6(4) determined by using NMR spectroscopy (see Supporting Information for details). The differences also do not appear to be due to a conformational equilibrium involving the dynamic behavior of the NHC ligand that is influenced by deuteration. For example, cooling solutions of **1-Cy** results in the freezing out of free rotation about the Ru-NHC carbon bond, rendering the *N*-mesityl groups inequivalent on the NMR timescale. The same behavior is observed upon cooling samples of [D_{11}]-**1-Cy**, but there is no measurable preference for the undeuterated mesityl group to occupy one environment over the other; the two inequivalent singlets for the mesityl aryl protons are present in a 1:1 ratio.[29] Furthermore, the intramolecular k_H/k_D measured for the symmetrical [D_6]-**1-R** isotopomers, where such an equilibrium effect would not be relevant, are identical to the intramolecular isotope effects measured in the [D_{11}]-isotopomers. It is possible that the discrepancy between the intra- and the intermolecular isotope effects is due to the effect of the various isotopic substitution patterns on unseen equilibria between intermediates **IV**–**VI**, but this remains a matter of speculation.

The important conclusion is that there is a substantial primary kinetic isotope effect that confirms that activation of a C–H bond in this position is the critical first step in the decomposition process in these compounds. Given the dynamic behavior of the NHC ligand, interaction of a benzylic C–H bond with the ruthenium center or the phosphonium alkylidene ligand directly would lead to significant ordering in the transition state, accounting for the large, negative $\Delta S^{\neq}$ observed.[30] The need to bring the C–H bond near to the metal center as a first step is also consistent with the observed faster decay rates for the sterically less bulky **1-*i*Pr** series of compounds.

Conclusions

The primary thermal decomposition mode of a family of highly active phosphonium alkylidene olefin metathesis catalysts was found to involve C–H activation of one of the N-heterocyclic carbene ligand's mesityl groups. This was supported by characterization of the decomposition product, and kinetic and labeling mechanistic studies. The implications of this observation for the further development of ligands for this family of catalysts are currently being considered. For example, N-heterocyclic carbene ligands that are less susceptible to C–H activation would be an obvious avenue to pursue.

Although this decomposition process is eventually detrimental to catalyst performance, it is worth noting that initiation rates for these catalysts are much faster than the rate-limiting step in the decomposition process identified here. Current studies are focusing on quantifying the initiation rates and determining the properties of the active propagating species.

Experimental Section

General: Argon-filled Innovative Technology System One dry boxes were used to store air- and moisture-sensitive compounds, and for the manipulation of air-sensitive materials. Reactions were performed either on a double manifold vacuum line using standard Schlenk techniques or under an argon atmosphere in the dry box for small-scale reactions. Glassware used in anhydrous reactions was stored in a hot oven (110 °C) overnight or flamed-dried prior to immediate use, and then transferred to the dry box. All non-deuterated starting materials were synthesized according to published procedures.[31] The syntheses of the deuterated complexes are given in the Supporting Information. Where applicable, cooling baths consisting of dry ice/acetone (−78 °C) were used to maintain low-temperature conditions. ^{1}H, ^{31}P{^{1}H}, ^{13}C{^{1}H}, ^{19}F, ^{11}B NMR experiments were performed on Bruker AMX-300, DMX-300, and DRX-400 spectrometers. Data are given in ppm relative to residual solvent signals for ^{1}H and ^{13}C. ^{19}F NMR spectra were referenced externally to C_6F_6 in C_6D_6 at $\delta = -163$ ppm relative to $CFCl_3$ at $\delta = 0.0$ ppm. ^{31}P NMR spectra were referenced to an aqueous external standard of H_3PO_4 in D_2O at $\delta = 0.0$ ppm. ^{11}B NMR spectra were referenced to $BF_3{\cdot}Et_2O$ in C_6D_6 at $\delta = 0.0$. Temperature calibration for high-temperature NMR experiments was achieved by monitoring the ^{1}H NMR spectrum of pure ethylene glycol before and after changing the temperature. For quantitative experiments 16 scans were collected for every spectrum. T_1 measurements were performed on the resonances of interest and a delay (d_1) of $5*T_1$ between single acquisitions was used, taking as a reference the longest relaxation time (in most cases a d_1 of 2 s was sufficient). Electrospray ionization mass spectrometry (ESI MS) was performed on the Bruker Esquire 3000 (positive mode, 3200 V capillary voltage, 7 psi nebulizer, 5.0 L min^{-1} dry gas, 300 °C dry temperature, 0.10 ms accumulation time, and target mass

set to 296 or 176 depending on phosphine). Quantitative experiments were prepared in triplicate and run in triplicate. A test for the capability of using ESI MS quantitatively for measuring a kinetic isotope effect was performed using known concentrations of $CH_3PCy_3^+$ and $CD_3PCy_3^+$ (see Supporting Information). Single-crystal X-ray diffraction was performed by Robert McDonald on a Bruker Platform/Smart 1000 CCD diffractometer (University of Alberta), and elemental anaylsis were performed on a Perkin–Elmer Model 2400, Series II, by Johnson Li (University of Calgary).

Decomposition kinetics by NMR spectroscopy (for Eyring plot, concentration variation, and intermolecular kinetic isotope effects): Compound **1-R-Cl** (25 mg, 0.028 mmol for **1-Cy-Cl** and 0.032 mmol for **1-*i*Pr-Cl**) was charged into a J-Young NMR tube along with $B(C_6F_5)_3$ (0.046 mmol for **1-Cy-Cl** and 0.054 mmol for **1-*i*Pr-Cl**), 1,1-dichloroethane (50 μL), $(CDCl_2)_2$ (0.4 mL), and an internal standard hexamethyldisiloxane (0.004 mmol). The tube was placed in an acetone/dry ice bath for transport to the NMR spectrometer and then placed in a pre-warmed NMR probe (70 °C for intermolecular kinetic isotope effects and a value between 40 °C–80 °C depending on the kinetic run). Proton cycling experiments were used to acquire spectra at various intervals during the decomposition (depending on the half-life), and the integration of the alkylidene proton ($\delta = 18$ ppm) against an internal standard ($\delta = 0.1$ ppm) was used for **1-Cy-Cl**. Integration of the methyl doublet of doublets (on the P*i*Pr$_3$ group) was used for **1-*i*Pr-Cl**, where the starting material was divided into the total integration of the starting material and decomposition product (methyl signal from the P*i*Pr$_3$ in the phosphonium salt).

Decomposition by ESI MS (intramolecular kinetic isotope effects): Compound [D_{11}]-**1-R-Cl** (25 mg, 0.028 mmol for [D_{11}]-**1-Cy-Cl** and 0.032 mmol for [D_{11}]-**1-*i*Pr-Cl**) was charged into a J-Young NMR tube along with $B(C_6F_5)_3$ (0.046 mmol for [D_{11}]-**1-Cy-Cl** and 0.054 mmol for [D_{11}]-**1-*i*Pr-Cl**), 1,1-dichloroethane (50 μL), and $(CDCl_2)_2$ (0.4 mL). The tube was heated by using an oil bath set to 70 °C on the benchtop. The reaction was monitored by ^{1}H and ^{31}P NMR spectroscopy, and deemed complete when the starting material ^{31}P NMR peak had completely disappeared, and the phosphonium salt decomposition product peak had appeared ($\delta = 61$ to 45 ppm for [D_{11}]-**1-*i*Pr**; $\delta = 55$ to 34 ppm for [D_{11}]-**1-Cy**). Once the reaction was complete, the solution was extracted with water (2.0 mL) to remove the $CD_nH_{3-n}PR_3^+$ salt mixture ($n = 0$–2, R = Cy, *i*Pr), which was directly measured in the ESI mass spectrometer. The intensity of the $CH_3PR_3^+$ peak (295 for R = Cy and 175 for R = *i*Pr) was divided by the corrected intensity (for the natural isotope pattern of the parent ion) of the $CHD_2PR_3^+$ peak (297 for R = Cy and 177 for R = *i*Pr) to provide the kinetic isotope effect.

Synthesis of 2: In a 50 mL reaction vessel, equipped with stir bar, **1-Cy-B-(C_6F_5)$_4$** (250 mg, 0.17 mmol) was added along with tetrachloroethane (5 mL) and 1,1-dichloroethene (1.25 mL, 16 mmol). The flask was sealed (with a Kontes tap), and heated to 70 °C in an oil bath overnight. The progress of the decomposition was monitored by ^{31}P{^{1}H} NMR spectroscopy by removal of an aliquot, concentration, and re-dissolving in CD_2Cl_2. Once all the starting material was decomposed (only one peak in the ^{31}P{^{1}H} NMR spectrum at $\delta = 34$ ppm), the reaction mixture was cooled and concentrated to dryness. The resulting brown residue was extracted with dichloromethane and water (to remove the phosphonium salt), and the organic extracts were combined and concentrated. The new residue was dissolved in a minimal amount of dichloromethane and layered with pentane. Red crystals were isolated and washed with pentane. Yield = 11 mg (6.5 %, 0.0056 mmol). ^{1}H NMR (399.6 MHz, $C_2D_2Cl_4$, 298 K; see Supporting Information for the spectrum): $\delta = 6.92$, 6.89, 6.77, 6.68 (s, 2H each; Mes C*H*), 5.03 (d, $^2J_{H,H(trans)} = 14$ Hz, $^2J_{H,H(gem)} = 0$ Hz, 2H; vinyl *H*), 4.66 (d, $^2J_{H,H(cis)} = 9$ Hz, $^2J_{H,H(gem)} = 0$ Hz, 2H; vinyl *H*), 4.22 (dd, $^2J_{H,H(cis)} = 9$ Hz, $^2J_{H,H(trans)} = 14$ Hz, 2H; vinyl *H*), 4.60, 4.12, 4.01, 3.78, (q, 2H each; NHC CH_2 backbone), 2.47, 2.30, 2.28, 2.25, 2.22 ppm (s, 6H each; Mes CH_3); ^{13}C{^{1}H} NMR (100.5 MHz, $C_2D_2Cl_4$, 298 K): $\delta = 264.42$ (s, CCl_2), 198.47 9S, NHC N*C*N), 139.61, 138.37, 137.69, 135.61, 134.89, 134.65, 134.33 (all s, Mes quaternary C), 134.01, 129.49, 128.97, 126.61 (s, Mes *C*H), 84.88, 79.39 (s, vinyl *C*), 56.45, 49.27 (s, NHC *C*H_2 backbone), 21.32, 20.62, 19.85, 19.23, 19.18 ppm (all s, Mes *C*H_3); ^{19}F NMR (282.4 MHz, $C_2D_2Cl_4$, 298 K): $\delta = -132.4$ (m, 8F; *ortho* C*F*), −162.2 (m, 4F; *para* C*F*), −166.1 ppm (m, 8F; *meta* C*F*); ^{11}B NMR (128.4 MHz, $C_2D_2Cl_4$, 298 K): $\delta = -16.15$ ppm (s, $B(C_6F_5)_4^-$); ESI MS for cationic dimer $C_{46}H_{52}Cl_7N_4Ru_2^+$: 1111 *m*/*z*; elemental analysis calcd (%) for $C_{70}H_{52}BCl_7F_{20}N_4Ru_2{\cdot}CH_2Cl_2$: C 45.48, H 2.90, N 2.99; found: C 45.88, H 3.04, N 2.92.

Generation of 3 in solution: Compound **1-*i*Pr-OTf** (or **1-*i*Pr**) (35 mg, 0.044 mmol) was charged into an NMR tube and CD_2Cl_2 (0.4 mL) was added. The tube was left at room temperature overnight (or for two nights for **1-*i*Pr**) and then was measured at the appropriate temperature in the NMR spectrometer. To prevent over decomposition long measurements were aquired at 220 K. Yield = 20 % (in solution). **1-*i*Pr-OTf** important peaks: ^{1}H NMR (399.6 MHz, CD_2Cl_2, 298 K): $\delta = 20.23$ (d, $^2J_{H,P} = 46$ Hz, 1H; RuC*H*P*i*Pr$_3$ in **3**), 18.57 (s, 1H; RuC*H*(NHC) in **3**), 18.38 ppm (d, $^2J_{H,P} = 39$ Hz, 1H; RuC*H*P*i*Pr$_3$ in **1**-*i*Pr-OTf); ^{1}H NMR (399.6 MHz, CD_2Cl_2, 220 K): $\delta = 20.09$ (d, $^2J_{H,P} = 45$ Hz, 1H; RuC*H*P*i*Pr$_3$ in **3**), 18.75 (d, $^2J_{H,P} = 44$ Hz, 1H; RuC*H*P*i*Pr$_3$ in **1-*i*Pr-OTf**), 18.43 ppm (s, 1H; RuC*H*(NHC) in **3**); ^{31}P{^{1}H} NMR (161.8 MHz, CD_2Cl_2, 298 K): $\delta = 54.33$ (br s, CH*Pi*Pr$_3$ in **1-*i*Pr-OTf**), 48.57 (s, CH*Pi*Pr$_3$ in **3**), 45.38 ppm (s, Me*Pi*Pr$_3$); ^{13}C NMR (from HMQC (no decoupling), 220 K): $\delta = 303.33$ (d, $^1J_{C,H} = 156$ Hz, Ru*C*H(NHC) in **3**), 292.29 (dd, $^1J_{C,H} = 166$ Hz, Ru*C*HP*i*Pr$_3$ in **3**), 271.43 ppm (dd, $^1J_{C,H} = 168$ Hz, RuC*H*P*i*Pr$_3$ in **1-*i*Pr-OTf**); $^1J_{C,P}$ couplings were not resolved. **1-*i*Pr** important peaks: ^{1}H NMR (399.6 MHz, CD_2Cl_2, 298 K): $\delta = 20.21$ (d, $^2J_{H,P} = 46$ Hz, 1H; RuC*H*P*i*Pr$_3$ in **3**), 18.57 (s, 1H; RuC*H*(NHC) in **3**), 17.77 ppm (d, $^2J_{H,P} = 35$ Hz, 1H; RuC*H*P*i*Pr$_3$ in **1-*i*Pr**); ^{1}H NMR (399.6 MHz, CD_2Cl_2, 220 K): $\delta = 20.08$ (d, $^2J_{H,P} = 45$ Hz, 1H; RuC*H*P*i*Pr$_3$ in **3**), 18.43 (s, 1H; RuC*H*(NHC) in **3**), 17.71 ppm (d, $^2J_{H,P} = 35$ Hz, 1H; RuC*H*P*i*Pr$_3$ in **1-*i*Pr**); ^{31}P{^{1}H} NMR (161.8 MHz, CD_2Cl_2, 298 K): $\delta = 60.95$ (s, CH*Pi*Pr$_3$ in **1-*i*Pr**), 48.40 (s, CH*Pi*Pr$_3$ in **3**), 45.24 ppm (s, Me*Pi*Pr$_3$); ^{13}C NMR (from HMQC (no decoupling), 220 K): $\delta = 303.35$ (d, $^1J_{C,H} = 171$ Hz, Ru*C*H(NHC) in **3**), 292.37 (dd, $^1J_{C,H} = 170$ Hz, Ru*C*HP*i*Pr$_3$ in **3**), 262.60 ppm (dd, $^1J_{C,H} = 178$ Hz, RuC*H*P*i*Pr$_3$ in **1-*i*Pr**); $^1J_{C,P}$ couplings were not resolved.

X-ray crystallography: X-ray crystallographic analysis of **2** was performed on suitable crystals coated in Paratone oil and mounted on a Bruker PLATFORM diffractometer/SMART 1000 CCD area detector system. CCDC-697188 (**2**) contains the supplementary crystallographic data for this paper. These data can be obtained free of charge from The Cambridge Crystallographic Data Centre via www.ccdc.cam.ac.uk/data_request/cif

Acknowledgements

Funding was provided by NSERC of Canada in the form of a Discovery Grant to W.E.P., and a CGSM scholarship to E.M.L.. Edwin van de Eide is acknowledged for useful discussions. Dr. Martine Monette (Bruker Canada) is gratefully acknowledged for performing ^{31}P{^{1}H} NMR experiments at 242.9 MHz in the analysis of $CH_nD_{3-n}PR_3^+$ isotopomers. Materia Inc. provided ruthenium catalysts.

[1] a) *Handbook of Metathesis* (Ed.: R. H. Grubbs), Wiley-VCH, Weinheim, **2003**; b) T. M. Trnka, R. H. Grubbs, *Acc. Chem. Res.* **2001**, *34*, 18–29; c) R. R. Schrock, C. Czekelius, *Adv. Synth. Catal.* **2007**, *349*, 55–77; d) Y. Chauvin, *Adv. Synth. Catal.* **2007**, *349*, 27–33.

[2] a) First-generation: P. Schwab, M. B. France, J. W. Ziller, R. H. Grubbs, *Angew. Chem, Int. Ed. Engl.* **1995**, *34*, 2039–2041; P. Schwab, R. H. Grubbs, J. W. Ziller, *J. Am. Chem. Soc.* **1996**, *118*, 100–110; b) second-generation: M. Scholl, S. Ding, C. W. Lee, R. H. Grubbs, *Org. Lett.* **1999**, *1*, 953–956; c) third-generation: M. S. Sanford, J. A. Love, R. H. Grubbs, *Organometallics* **2001**, *20*, 5314–5318; d) Hoveyda–Grubbs: J. S. Kingsbury, J. P. A. Harrity, P. J. Bonitatebus, Jr., A. H. Hoveyda, *J. Am. Chem. Soc.* **1999**, *121*, 791–799; S. B. Garber, J. S. Kingsbury, B. L. Gray, A. H. Hoveyda, *J. Am. Chem. Soc.* **2000**, *122*, 8168–8179.

[3] a) K. M. Kuhn, R. H. Grubbs, *Org. Lett.* **2008**, *10*, 2075–2077; b) G. C. Vougioukalakis, R. H. Grubbs, *J. Am. Chem. Soc.* **2008**, *130*,

2234–2245; c) I. C. Stewart, C. J. Douglas, R. H. Grubbs, *Org. Lett.* **2008**, *10*, 441–444; d) G. C. Vougioukalakis, R. H. Grubbs, *Organometallics* **2007**, *26*, 2469–2472; e) S. Monfette, D. E. Fogg, *Organometallics* **2006**, *25*, 1940–1944; f) J. C. Conrad, D. Amoroso, P. Czechura, G. P. A. Yap, D. E. Fogg, *Organometallics* **2003**, *22*, 3634–3636; g) L. Jafarpour, H.-J. Schanz, E. D. Stevens, S. P. Nolan, *Organometallics* **1999**, *18*, 5416—5419; h) V. Dragutan, I. Dragutan, F. Verpoort, *Platinum Met. Rev.* **2005**, *49*, 33–40; i) M. Bieniek, A. Michrowska, D. L. Usanov, K. Grela, *Chem. Eur. J.* **2008**, *14*, 806–818; j) K. Grela, S. Harutyunyan, A. Michrowska, *Angew. Chem.* **2002**, *114*, 4210–4212; *Angew. Chem. Int. Ed.* **2002**, *41*, 4038–4040; k) H. Wakamatsu, S. Blechert, *Angew. Chem.* **2002**, *114*, 832–834; *Angew. Chem. Int. Ed.* **2002**, *41*, 794–796.

[4] a) E. L. Dias, S. T. Nguyen, R. H. Grubbs, *J. Am. Chem. Soc.* **1997**, *119*, 3887–3897; b) M. S. Sanford, M. Ulman, R. H. Grubbs, *J. Am. Chem. Soc.* **2001**, *123*, 749–750; c) M. S. Sanford, J. A. Love, R. H. Grubbs, *J. Am. Chem. Soc.* **2001**, *123*, 6543–6554.

[5] See [3a, 3i] and a) I. C. Stewart, T. Ung, A. A. Pletnev, J. M. Berlin, R. H. Grubbs, Y. Schrodi, *Org. Lett.* **2007**, *9*, 1589–1592; b) A. Fürstner, L. Ackermann, B. Gabor, R. Goddard, C. W. Lehmann, R. Mynott, F. Stelzer, O. R. Thiel, *Chem. Eur. J.* **2001**, *7*, 3236–3253.

[6] a) D. R. Anderson, D. J. O'Leary, R. H. Grubbs, *Chem. Eur. J.* **2008**, *14*, 7536–7544; b) D. R. Anderson, D. D. Hickstein, D. J. O'Leary, R. H. Grubbs, *J. Am. Chem. Soc.* **2006**, *128*, 8386–8387; c) A. G. Wenzel, R. H. Grubbs, *J. Am. Chem. Soc.* **2006**, *128*, 16048–16049; d) T. Ung, A. Hejl, R. H. Grubbs, Y. Schrodi, *Organometallics* **2004**, *23*, 5399–5401; e) M. S. Sanford, L. M. Henling, M. W. Day, R. H. Grubbs, *Angew. Chem.* **2000**, *112*, 3593–3595; *Angew. Chem. Int. Ed.* **2000**, *39*, 3451–3453; f) J. A. Tallarico, P. J. Bonitatebus, Jr., M. L. Snapper, *J. Am. Chem. Soc.* **1997**, *119*, 7157–7158.

[7] a) A. Correa, L. Cavallo, *J. Am. Chem. Soc.* **2006**, *128*, 13352–13353; b) C. Aldhart, P. Chen, *Angew. Chem.* **2002**, *114*, 4668–4671; *Angew. Chem. Int. Ed.* **2002**, *41*, 4484–4487; c) B. F. Straub, *Angew. Chem.* **2005**, *117*, 6129–6132; *Angew. Chem. Int. Ed.* **2005**, *44*, 5974–5978; d) C. H. Suresh, M.-H. Baik, *Dalton Trans.* **2005**, 2982–2984; e) D. Benitez, W. A. Goddard III, *J. Am. Chem. Soc.* **2005**, *127*, 12218–12219; f) C. H. Suresh, N. Koga, *Organometallics* **2004**, *23*, 76–80; g) C. Adlhart, P. Chen, *J. Am. Chem. Soc.* **2004**, *126*, 3496–3510; h) J. Oxgaard, W. A. Goddard III, *J. Am. Chem. Soc.* **2004**, *126*, 442–443; i) S. F. Vyboishchikov, M. Bühl, W. Thiel, *Chem. Eur. J.* **2002**, *8*, 3962–3975.

[8] a) P. E. Romero, W. E. Piers, R. McDonald, *Angew. Chem.* **2004**, *116*, 6287–6291; *Angew. Chem. Int. Ed.* **2004**, *43*, 6161–6165; b) S. R. Dubberley, P. E. Romero, W. E. Piers, R. McDonald, M. Parvez, *Inorg. Chim. Acta* **2006**, *359*, 2658–2664.

[9] P. E. Romero, W. E. Piers, *J. Am. Chem. Soc.* **2005**, *127*, 5032–5033.

[10] a) S. Torker, D. Merki, P. Chen, *J. Am. Chem. Soc.* **2008**, *130*, 4808–4814; b) C. Adlhart, P. Chen, *Helv. Chim. Acta* **2003**, *86*, 941–949; c) C. Adlhart, M. A. O. Volland, P. Hofmann, P. Chen, *Helv. Chim. Acta* **2000**, *83*, 3306–3311; d) C. Adlhart, P. Chen, *Helv. Chim. Acta* **2000**, *83*, 2192–2196.

[11] E. F. van der Eide, P. E. Romero, W. E. Piers, *J. Am. Chem. Soc.* **2008**, *130*, 4485–4491.

[12] P. E. Romero, W. E. Piers, *J. Am. Chem. Soc.* **2007**, *129*, 1698–1704.

[13] M. Ulman, R. H. Grubbs, *J. Org. Chem.* **1999**, *64*, 7202–7207.

[14] a) J. C. Conrad, J. L. Snelgrove, M. D. Eelman, S. Hall, D. E. Fogg, *J. Mol. Catal. A* **2006**, *254*, 105–110; b) J. C. Conrad, D. E. Fogg, *Curr. Org. Chem.* **2006**, *10*, 185–202; c) A. H. Hoveyda, D. G. Gillingham, J. J. van Veldhuizen, O. Kataoka, S. B. Garber, J. S. Kingsbury, J. P. A. Harrity, *Org. Biomol. Chem.* **2004**, *2*, 8–23.

[15] K. Tanaka, V. P. W. Böhm, D. Chadwick, M. Roeper, D. C. Braddock, *Organometallics* **2006**, *25*, 5696–5698.

[16] a) D. Banti, J. C. Mol, *J. Organomet. Chem.* **2004**, *689*, 3113–3116; b) M. B. Dinger, J. C. Mol, *Organometallics* **2003**, *22*, 1089–1095; c) M. B. Dinger, J. C. Mol, *Eur. J. Inorg. Chem.* **2003**, 2827–2833; d) J. Louie, R. H. Grubbs, *Organometallics* **2002**, *21*, 2153–2164.

[17] a) B. R. Galan, M. Pitak, J. B. Keister, S. T. Diver, *Organometallics* **2008**, *27*, 3630–3632; b) B. R. Galan, K. P. Kalbarxzyk, S. Szczepankiewicz, J. R. Keister, S. T. Diver, *Org. Lett.* **2007**, *9*, 1203–1206; c) B. R. Galan, M. Gembicky, P. M. Dominiak, J. B. Keister, S. T. Diver, *J. Am. Chem. Soc.* **2005**, *127*, 15702–15703.

[18] a) S. H. Hong, A. G. Wenzel, T. T. Salguero, M. W. Day, R. H. Grubbs, *J. Am. Chem. Soc.* **2007**, *129*, 7961–7968; b) S. H. Hong, R. H. Grubbs, *J. Am. Chem. Soc.* **2004**, *126*, 7414–7415.

[19] See ref. [11] and M. L. Macnaughtan, M. J. A. Johnson, J. W. Kampf, *J. Am. Chem. Soc.* **2007**, *129*, 7708–7709.

[20] W. E. Piers, *Adv. Organomet. Chem.* **2005**, *52*, 1–77.

[21] A. K. Chatterjee, T.-L. Choi, D. P. Sanders, R. H. Grubbs, *J. Am. Chem. Soc.* **2003**, *125*, 11360–11370.

[22] Monohalogen-substutituted olefins react with compounds **1** and other ruthenium-based olefin metathesis initiators: See ref. [19] and M. L. Macnaughtan, M. J. A. Johnson, J. W. Kampf, *Organometallics* **2007**, *26*, 780–782.

[23] See reference [1a], page 92. The ^{13}C NMR shift for a similar difluorocarbene monomeric complex is $\delta = 218.09$ ppm: T. M. Trnka, M. W. Day, R. H. Grubbs, *Angew. Chem.* **2001**, *113*, 3549–3552.

[24] Other literature precedence for C–H activation includes: a) S. H. Hong, A. Chlenov, M. W. Day, R. H. Grubbs, *Angew. Chem.* **2007**, *119*, 5240–5243; *Angew. Chem. Int. Ed.* **2007**, *46*, 5148–5151; b) T. M. Trnka, J. P. Morgan, M. S. Sanford, T. E. Wilhelm, M. Scholl, T.-L. Choi, S. Ding, M. W. Day, R. H. Grubbs, *J. Am. Chem. Soc.* **2003**, *125*, 2546–2558; c) R. F. R. Jazzar, S. A. Macgregor, M. F. Mahon, S. P. Richards, R. H. Grubbs, *J. Am. Chem. Soc.* **2002**, *124*, 4944–4945.

[25] K. Vehlow, S. Gessler, S. Blechert, *Angew. Chem.* **2007**, *119*, 8228–8231; *Angew. Chem. Int. Ed.* **2007**, *46*, 8082–8085.

[26] The affect of the counteranion on the rate and mechanism of these decompositions has not been studied in detail, nor is it well understood. Here, substitution of the borate counteranion for the triflate renders the self trapping process to generate **3** more rapidly; at this point, this is simply an empirical observation.

[27] a) The ^{13}C NMR shift for a similar *ortho*-chelating aryl on the NHC is $\delta = 292.6$ ppm: D. Burtscher, B. Perner, K. Mereiter, C. Slugovc, *J. Organomet. Chem.* **2006**, *691*, 5423–5430; b) a second-generation Grubbs catalyst has a $^{1}J_{C,H}$ value of 148 Hz: S. Leuthäußer, V. Schmidts, C. M. Thiele, H. Plenio, *Chem. Eur. J.* **2008**, *14*, 5465.

[28] E. L. Dias, R. H. Grubbs, *Organometallics* **1998**, *17*, 2758–2767.

[29] See ref. [8a]. The barrier for rotation about the Ru–NHC bond is very low at 11.5(5) kcal mol^{-1}. Ru-NHC bond rotation barriers of 21–22 kcal mol^{-1} are observed in second-generation Grubbs' systems, see reference [27b].

[30] Even a strongly ordered transition state does not fully account for the magnitude of the entropy of activation. However, we note that these are ionic compounds and solvent cage reorganization may contribute significantly to this part of the barrier.

[31] For the syntheses of **1-Cy-Cl**, **1-*i*Pr-Cl**, and **1-*i*Pr-OTf** see ref. [19]; and for the synthesis of **1-Cy-B(C_6F_5)$_4$** see ref. [8a].

Received: August 1, 2008
Published online: November 26, 2008

